

# Combined Impacts of ENSO and MJO on the 2015 Growing Season Drought over the Canadian Prairies

Zhenhua Li<sup>1,2</sup>, Yanping Li<sup>1</sup>, Barrie Bonsal<sup>3</sup>, Alan H. Manson<sup>2</sup>, Lucia Scaff<sup>1</sup>

<sup>1</sup>Global Institute for Water Security, University of Saskatchewan, Saskatoon, Saskatchewan, Canada S7N3H5

<sup>2</sup>Institute of Space and Atmospheric Studies, University of Saskatchewan, Saskatoon, Saskatchewan, Canada

<sup>3</sup>National Hydrology Research Center, Environment and Climate Change Canada, Saskatoon, SK, Canada

*Correspondence to:* Dr. Yanping Li (yanping.li@usask.ca); Dr. Zhenhua Li (zhenhua.li@usask.ca)

## Abstract

Warm-season precipitation over the Canadian Prairies plays a crucial role in activities, environment and society and has particular importance to agricultural production over the region. This research investigates how a warm season precipitation deficit over the Canadian Prairies is related to tropical Pacific forcing in the early summer 2015 drought. The significant deficit of precipitation in May and June of 2015 were coincident with a warm phase of El Niño-Southern Oscillation (ENSO) and a negative phase of Madden-Julian Oscillation (MJO)-4 index as they favor a positive geopotential height anomaly in western Canada. Further investigation during the instrumental record period (1979-2015) shows that the warm-season precipitation in the Canadian Prairies and the corresponding atmospheric circulation anomalies over western Canada teleconnected with the lower boundary conditions in the tropical western Pacific. MJO may play a crucial role in determining the summer precipitation anomaly in the western Canadian Prairie when equatorial central Pacific is warmer than normal (NINO4 > 0) and MJO is more active. The mechanism of this teleconnection may be due to the propagation of stationary Rossby wave that is generated in the MJO-4 index region. When the tropical convection around MJO-4 index regions (western tropical Pacific, centered over 140°E) is more active than normal when NINO4 > 0, a Rossby wave train originates from western Pacific and propagates into the midlatitude North America causing an anomalous ridge in the upper level over western Canada.

## 23 **1 Introduction**

24 The Canadian Prairies are highly dependent on summer precipitation especially during the early  
25 to mid-growing season (May through July) when the majority of annual precipitation normally occurs  
26 (Bonsal et al. 1993). High natural variability in growing season precipitation causes periodic  
27 occurrences of extreme precipitation (Li et al. 2017) and droughts that are often associated with reduced  
28 agriculture yields, low stream flow, and increased occurrence of forest fires (Wheaton et al. 2005,  
29 Bonsal and Regier 2007). Drought events with great environmental and economic impacts have  
30 occurred in 1961, 1988, 2001-2002, and as recent as 2015 (Dey 1982, Liu et al. 2004, Bonsal et al.  
31 1999, Wheaton et al. 2005, Shabbar et al. 2011, Bonsal et al. 2013, Szeto et al. 2016). The sub-seasonal  
32 forecasting of precipitation during the growing season are crucial for the agriculture, water resource  
33 management, and the economy in the region. Therefore, an investigation into the potential causes of the  
34 inter-annual variability of growing season precipitation of the Canadian Prairie is much needed to  
35 provide important information for the **agriculture and economy** in the region.

36 Low precipitation and extended dry periods on the Canadian Prairies are often associated with  
37 upper-level ridge and a persistent high pressure centered over the Prairies (Dey 1982, Liu et al. 2004).  
38 These prolonged atmospheric anomalies often concurred with abnormal boundary conditions such as  
39 large-scale sea surface temperature (SST) anomalies in the Pacific (Shabbar and Skinner 2004). Large  
40 scale oscillation in the SST anomalies in Pacific Ocean, namely El Nino, the Pacific **Decadal**  
41 Oscillation (PDO), can affect the hydroclimatic pattern in North America, although the strongest  
42 impacts of these boundary conditions occur during the boreal winter. Inter-annual variabilities such as  
43 El Nino-Southern Oscillation (ENSO) events are found to be linked with extended droughts in the  
44 Prairies (Bonsal et al. 1999, Shabbar and Skinner 2004). Interdecadal oscillation such as the PDO, and

45 the Atlantic Multi-decadal Oscillation (AMO) have also been found to affect the seasonal temperature  
46 and precipitation in the Canadian Prairies (Shabbar et al. 2011).

47 ENSO's relationship with the Canadian Prairies' precipitation has been studied extensively. The  
48 warm phase of ENSO often favours drought in the Canadian Prairies, especially during the growing  
49 season after the mature phase of El Nino with North Pacific Mode (ENPM) like North Pacific SST  
50 anomaly pattern (Bonsal and Lawford 1999, Shabbar and Skinner 2004). Previous investigations (e.g.,  
51 Shabbar *et al.* (2011)) have found El Nino events are associated with a summer moisture deficit in the  
52 western Canada while La Nina events cause an abundance of moisture in extreme western Canada  
53 (British Columbia and Yukon). However, they also noted that although tropical SST variability  
54 accounted for some aspects of the large-scale circulation anomalies that influence Canadian Prairies  
55 drought, a consistent and clear-cut relationship was not found. North Pacific SST warm anomalies,  
56 which often follow a matured El Nino, and accompanying atmospheric ridging leads to extended dry  
57 spells over the Prairies during the growing season (Bonsal and Lawford 1999). For the recent North  
58 Pacific SST anomaly from 2013 to 2014, researchers have attributed the precipitation deficit in  
59 California during 2013 to the anomalous upper-level ridge over the western North America (Wang *et al.*  
60 2014, Szeto et al. 2016).

61 The formerly mentioned SST variations (ENSO, PDO, etc.) mostly vary on interannual and  
62 decadal scales. Another important factor that affects the weather patterns in North America is the  
63 Madden-Julian Oscillation (MJO), an intra-seasonal (40-90 days) oscillation in convection and  
64 precipitation pattern in the Tropics (Zhang 2005, Madden and Julian 1971, Riddle *et al.* 2013, Carbone  
65 and Li 2015). MJO is a coupled atmosphere-ocean oscillation involving convections and large-scale  
66 equatorial waves, which produces an eastward movement of tropical convection anomaly on an  
67 intraseasonal scale (Madden and Julian 1971). MJO has been found to affect the winter temperature and

68 precipitation in North America and Europe through its impact on moisture transport associated with  
69 “Pineapple Express” and its effects on North Atlantic Oscillation and stratospheric polar vortex (Cassou  
70 2008, Garfinkel *et al.* 2012, Rodney *et al.* 2013). MJO has been found to be connected to precipitation  
71 anomalies to summer precipitation in the Southwest United States (Lorenz and Hartmann 2006). During  
72 spring and summer, MJO's impact on the Canadian Prairies' precipitation has not been thoroughly  
73 investigated as MJO's amplitude is weak during summer. The amplitude of MJO in spring and early  
74 summer, however, is related to the interannual variation of tropical SST, especially the SST in central  
75 Pacific (Hendon *et al.* 2007, Marshall *et al.* 2016). The amplitude of MJO in terms of the Real-time  
76 Multivariate MJO index (RMM, Wheeler and Hendon 2004) was extremely strong in the early spring of  
77 2015 with high SST anomaly in the central Pacific and El Nino became strong.

78 MJO activities in the western Pacific under the modulation of interannual variability of SST have  
79 the potential to act together and impact mid-tropospheric circulation over western Canada and thus,  
80 warm season precipitation over the Canadian Prairies. The goal of the study is to demonstrate that the  
81 mechanism involved MJO may cause the meteorological drought in growing season in the Canadian  
82 Prairies in 2015. Subsequently, further investigations are carried out to determine if similar relationships  
83 exist in association with other summer extreme precipitation events during instrumental record (1979-  
84 2016). Section 2 provides the datasets and methodologies used in this paper while section 3 presents  
85 analyses of the upper-level circulation anomaly and SST pattern associated with the 2015 drought. This  
86 is followed by examination of the effects of central Pacific SST anomaly and MJO on the summer  
87 precipitation in the Canadian Prairies using data during instrumental record period. The potential  
88 mechanism by which MJO affects summer precipitation when equatorial central Pacific SST is warmer  
89 than normal is discussed in section 4 followed by a summary of the results and concluding remarks in  
90 section 5.

## 91 **2 Data and Methodology**

### 92 **2.1 Data**

93

94 Multiple observation and reanalysis datasets are used to investigate the circulation anomalies  
95 associated with Canadian Prairie growing season (May-August) precipitation. Observed precipitation is  
96 taken from the Climate Prediction Center (CPC) Merged Analysis of Precipitation (CMAP) dataset (Xie  
97 and Arkin 1997). Geopotential height fields include those from the National Center for Environmental  
98 Predictions (NCEP) Reanalysis (Kalnay *et al.* 1996) and the European Center for Medium-Range  
99 Weather Forecast (ECMWF)'s ERA-interim (Dee *et al.* 2011), and are used to analyze upper-level (200  
100 hPa and 500 hPa) atmospheric circulation patterns.

101 To represent the central Pacific SST anomaly, NINO4 SST index (Rayner *et al.* 2003) from CPC  
102 of National Oceanic and Atmospheric Administration (NOAA) is used since the NINO4 region is near  
103 central Pacific and spans over the dateline (5°S-5°N, 160°E-150°W). Multivariate ENSO Index (MEI)  
104 data are retrieved from National Oceanic and Atmospheric Administration (NOAA)'s Climate Data  
105 Center (CDC) website and are used to determine the ENSO phase (Wolter 1987, Wolter and Timlin  
106 1993). In particular, an El Nino condition is defined when the monthly mean index of MEI is larger than  
107 0.5 as it identifies El Nino events consistently (Andrews *et al.* 2004).

108 The Real-time Multivariate MJO series (RMM1 and RMM2) developed by Wheeler and Hendon  
109 (2004) are used to identified the periods of strong MJO activities as the MJO amplitudes are readily  
110 available by the calculation of the square root of RMM1 + RMM2. For MJO intensities in a region, we  
111 used the monthly averaged pentad MJO indices from NOAA CPC's MJO index (Xue *et al.* 2002) which  
112 have 10 indices representing locations around the globe. The CPC's MJO index is based on Extended

113 Empirical Orthogonal Function (EEOF) analysis on pentad velocity potential at 200-hPa. Ten daily MJO  
114 indices are constructed by projecting the daily (00Z) velocity potential anomalies at 200-hPa (CHI200)  
115 onto the ten time-lagged patterns of the first EEOF of pentad CHI200 anomalies (Xue *et al.* 2002).  
116 Negative values of ten MJO indices correspond to enhanced convections to 10 regions centered on  
117 20°E, 70°E, 80°E, 100°E, 120°E, 140°E, 160°E, 120°W, 40°W and 10°W in the tropics. A negative  
118 value of the CPC's MJO indices (usually varies between -2 to 2) indicates an above average convective  
119 activities in the corresponding region. Because boreal summer corresponds to a period of weaker  
120 amplitude of MJO than winter, we choose monthly mean value of -0.3 as the criterion of strong  
121 convections that are connected to MJO. The monthly mean MJO-4 index less than -0.3 is the criterion  
122 considered as a relatively strong convection associated with MJO in the western Pacific where has been  
123 found to be a source region of stationary Rossby waves (Simmons 1980). SST observations include  
124 Extended Reconstructed Sea Surface Temperature (ERSST) v4 (Huang *et al.* 2015). Outward Longwave  
125 Radiation (OLR) data from NOAA Interpolated Outgoing Longwave Radiation (hosted at  
126 <http://www.esrl.noaa.gov/psd/map/clim/olr.shtml>) are used to derived the composite anomalous field of  
127 OLR for a certain phase of MJO as described below.

128

129

### 130 **3 Results**

131 This study focuses on the growing season precipitation in the provinces of Alberta and Saskatchewan in  
132 the Canadian Prairies, where the largest deficits were observed in 2015. Specifically, the regional mean  
133 precipitation over 115°-102.5°W, 50°-57.5°N is used (boxed arear in Figure 1) to represent the

134 Canadian Prairies east of the Rocky Mountains and south of the boreal forest. The region chosen also  
135 covers most of the arable land in the Canadian Prairies for datasets with 2.5-degree resolution. As the  
136 indicated by the MJO-4 and NINO4 index for 2015, the relationship between the Prairies' warm season  
137 (May-August) precipitation with MJO-4 and ENSO during the instrumental records are investigated  
138 using correlation and regression. The possible mechanism behind the correlation between MJO-4 and  
139 the Prairie's warm season precipitation during El Nino condition is further investigation by analyzing  
140 the upper-level circulation associated with convections in the Tropics and stationary Rossby waves in  
141 the midlatitudes. 

142

### 143 **3.1 The 2015 Summer Drought**

144 Almost all of western Canada including British Columbia, the southern Northwest Territories,  
145 Alberta and Saskatchewan had significant negative precipitation anomalies during May and June 2015.  
146 The warm season precipitation is represented by the monthly mean precipitation from May to August  
147 (Bonsal *et al.* 1999, Shabbar *et al.* 2011). For the 2015 case study, during May-June, the **prairies'**  
148 precipitation was significantly below average. The top plot in Fig. 1 shows the precipitation anomaly in  
149 percentage relative to climatology (1981-2010 long term mean) in Canada during May and June 2015.  
150 The bottom plot in Fig. 1 presents the monthly precipitation anomaly averaged over the region  
151 encompassed by the dash lines (50N-57.5N, 115W-102.5W). The annual cycle of the regional  
152 precipitation has, **in** average, a dry period between February and May. Regarding the precipitation  
153 climatology, June has the largest precipitation in all months with significantly more rain than  
154 neighboring months. When both May and June 2015 **witness** much less precipitation than normal in  
155 addition to a relatively dry period from February to April, the region gets little precipitation.

156 Fig. 1 Top: Precipitation anomalies (mm) from CMAP over the region (115 W-102.5 W, 50 N-57.5 N) during May  
157 and June 2015. Bottom: time series of monthly precipitation anomaly over boxed region between September 2013 and  
158 August 2015.

159 The upper-level geopotential height anomaly averaged in May and June are examined together  
160 with SST anomaly and ENSO, MJO-4 indices for 2014 and 2015. The 500 hPa geopotential height  
161 (GPH) anomaly for the May and June 2015 shows strong positive anomalies near Alaska and British  
162 Columbia coast in Fig. 2, which is consistent with the findings for other growing season droughts (e.g.,  
163 Dey 1982; Bonsal and Wheaton, 2005). Accompanying this anomalous ridge extending from Alaska to  
164 Pacific Northwest of the US is an above normal warm SST in the northeast Pacific off the coast of North  
165 America and the central-eastern Pacific (Fig. 3). Both ENSO and North Pacific Mode (NPM) (Hartmann  
166 et al. 2015) are in positive phases that corresponds to a warmer SST near the Pacific coast of North  
167 America, consistent with the positive GPH anomalies in western Canada and Alaska. The ridge in  
168 Alaska/Bering Straits and the one near British Columbia coast are associated with El Nino and North  
169 Pacific SST anomaly such as NPM (Shabbar *et al.* 2011). The monthly mean anomalous ridge indicates  
170 a tendency to prevent storms from reaching the British Columbia coast and the Canadian Prairies  
171 causing extended dry spells. The GPH anomaly in early growing season in 2015 is consistent with the  
172 precipitation anomaly in these regions. The anomalous upper-level ridge in the Western United States  
173 and Canada in 2014 and 2015 have also been associated with the developing El Nino and the other main  
174 components of Pacific sea surface temperature (SST) variation such as NPM by several recent studies  
175 (Hartmann 2015, Lee *et al.* 2015, Li et al. 2017).

176 Fig. 2 NCEP GPH anomaly at 500hPa during May and June 2015 when the precipitation deficit was the largest.

177 Fig. 3 shows the average SST anomaly during the growing season (May-August) of 2015. The  
178 strong positive anomaly in the Northeast Pacific and eastern equatorial Pacific is evident and persistent

179 through the summer, which corresponds to the warm phase of NPM and ENSO, respectively. SST in the  
180 eastern tropical Pacific warms increasingly since the end of 2014 and qualifies as an El Nino in early  
181 2015. The NPM becomes positive since fall 2013 and turns to exceptionally strong in 2014 and persist  
182 to 2015 (Hartmann 2015). The anomalous ridge is concurrent with strong SST anomalies in both  
183 tropical Pacific and extratropical North Pacific. NPM, as the third EOF of Pacific SST (30S-65N), also  
184 has a strong connection to the anomalous ridge in the western North America and trough in the eastern  
185 US and Canada in 2013-2014 winter (Hartmann 2015, Lee *et al.* 2015). During the ENSO-neutral  
186 condition in 2013 and 2014, the precursor of ENSO, so-called "footprinting" mechanism is considered  
187 by some researchers to cause this anomalous ridge in the western North America (Wang *et al.* 2014).

188 Summer of 2015 is the first summer after the developing El Nino during 2014-2015 winter.  
189 Though the upper-level GPH pattern seen in summer 2015 can be attributed to the SST modes in the  
190 Pacific Basin, namely ENSO and NPM, the precipitation in the Western Canadian Prairie is not strongly  
191 correlated with either of them. Bonsal and Lawford (1999) found that more extended dry spells tend to  
192 occur during the second summer following the mature stage of the El Nino events. The winter  
193 precipitation in Canada has been shown to have a strong connection to ENSO (Shabbar *et al.* 1997),  
194 whereas summer precipitations in most regions of western Canada (except the coast of British Columbia  
195 and Southern Alberta) do not have significant correlations with ENSO. This is consistent with our  
196 investigation using instrumental records from 1948 to 2016.

197 The variation of the Canadian Prairies' precipitation and its relationship with SST modes and  
198 MJOs shown in Fig. 4. The time series of monthly RMM amplitude anomaly, NINO4 index, MJO-4  
199 indices and the Canadian Prairies precipitation anomaly from January 2014 to December 2015 shows  
200 the atmospheric-oceanic circulation condition for the drought in 2015. In 2015 both May and June saw a  
201 strong MJO-4 negative indices, whereas in July the MJO-4 index became positive. This corresponds

202 quite well with the precipitation anomaly in Fig. 1. As shown in Fig. 3, the 0El Nino continued to  
203 strengthen in July and August 2015; in the meantime, the MJO-4 index increased in July and August  
204 2015. The increase of MJO-4 index corresponded to the active convections associated with MJO in  
205 West Pacific propagated eastward into the central Pacific; the precipitation in the Canadian Prairie  
206 returned to slightly above normal in July.

207           The good correspondence of MJO-4 index and negative precipitation anomaly suggests a link  
208 between MJO related tropical convection anomaly and the prairie precipitation during growing season.  
209 Though El Nino and associated Northeast Pacific warm anomaly (i.e., NPM) in summer 2015 can be a  
210 contributing factor for the upper-level ridge on the west coast of Canada, it cannot fully explain the  
211 drought condition in West Canada as these SST conditions **does** not guarantee a prolonged dry spell as  
212 shown by correlation analysis. The negative MJO-4 index concurred with the negative anomaly of  
213 Prairie precipitation in 2015, which prompts the investigation of their relationship in the instrumental  
214 records.

215 Fig. 3 The mean SST anomaly(°C) from ERSST v4 in May-August 2015.

216 Fig. 4 RMM amplitude anomaly, NINO4, MJO 4 indices and precipitation anomaly of Canadian Prairies from January 2014  
217 to Dec 2015.

218

## 219 **3.2 Instrumental record**

220           El Nino and its associated North Pacific SST anomaly may contribute to extended dry spells in  
221 Canadian Prairies after the matured phase of El Nino (Bonsal et al. 1993) on an interannual time scale.  
222 ENSO, however, is not a strong intra-seasonal to seasonal predictor of Canadian Prairie summer  
223 precipitation. Here we present a new result showing that under warm central Pacific SST condition

224 (NINO4 >0), a certain phase of MJO, which connected to the active convections in the tropical western  
225 Pacific (Li and Carbone 2012), plays an important role to determine the precipitation in the Canadian  
226 Prairies in the early summer months.

227 Table 1 Correlation between mean precipitation anomaly from CMAP in the prairie and MEI, MJO indices 4. MJO  
228 indices and are from 1979 to 2016. CMAP covers 1979 to 2016.

229

230 The correlation coefficients between the mean regional precipitation anomaly over Canadian  
231 Prairies and MJO-4 indices and MEI from May to August are shown in Table 1. The correlation  
232 between MEI and the precipitation anomalies is not significant. The negative MJO-4 index represents a  
233 stronger than normal convection in the Maritime Continents and the tropical Western Pacific. The  
234 correlation between MJO-4 index and precipitation in the Prairies indicates that stronger tropical  
235 convections in the Equatorial region centered around 140°E favor less precipitation in the Canadian  
236 Prairies from May to August. The correlation between MJO-4 index and the growing season Prairie  
237 precipitation anomaly is 0.18 with a p-value of 0.023. The correlation between MJO-4 index and the  
238 precipitation anomaly during growing season when NINO4 >0 is much higher at 0.33 with a p-value of  
239 0.0015. The correlation between MJO-4 and the Canadian Prairie precipitation when NINO4 < 0 is -  
240 0.01.

241 Fig. 5 The scatterplot of monthly precipitation anomaly (mm/month) as a function of MJO-4 and NINO4. Each  
242 asterisk represents a month from May to August 1979-2016. Circled asterisk denotes a month with precipitation anomaly  
243 larger than 18 mm/month. The blue circles are months with positive precipitation anomaly and the red circles are months with  
244 negative precipitation anomaly. The sizes of circles denote the magnitudes of the anomalies (large > 30 mm/month, medium >  
245 24 mm/month, small >18 mm/month). The shaded area denotes NINO4>0 and MJO-4 index < 0.

246 The scatter plot in Fig. 5 shows the distribution of monthly precipitation anomaly versus MJO-4  
247 index and NINO4 index, which together affect the precipitation anomaly from May to August. Circled  
248 asterisk denotes a month with precipitation anomaly larger than 18 mm/month and the red (blue) circles  
249 denote negative (positive) precipitation. The sizes of the circle represent the magnitude of the monthly  
250 precipitation anomalies. In the bottom-right region indicated by shading, under NINO4 > 0 condition,  
251 negative MJO-4 corresponds to many more dry months than wet months. We noticed that some  
252 significant dry months are not in the shaded region which corresponds to the dry months occur in La  
253 Nina condition or in the period after the mature phase of El Nino (Bonsal et al. 1999).

254 Fig. 6 The box-percentile plot of Canadian Prairies precipitation anomaly during growing season for ENSO  
255 conditions.

256 To investigate the impact of ENSO on the growing season precipitaiton over Canadian Prairies,  
257 the distribution of precipitation anomaly along ENSO conditions are plotted. The box-percentile plot in  
258 Fig. 6 shows the distribution of monthly Canadian Prairies' precipitation anomalies from May to August  
259 along ENSO condition. In general, under El Nino and ENSO neutral condition the precipitation  
260 anomalies centered on 0, and there is no bias toward either end. Under La Nina condition, the mean  
261 precipitation has a positive bias. There are only 10 summer months under La Nina condition, whereas  
262 both El Nino and neutral condition have 71 months.

263 The distributions of precipitation anomalies versus MJO-4 index under different ENSO  
264 conditions are shown in Fig. 7. Under warm central Pacific SST condition (NINO4 >0), the precipitation  
265 anomaly has a negative tendency for MJO-4 < -0.3. Under NINO4 >0 condition, there is no such  
266 negative tendency for the precipitation anomaly under the condition of MJO-4 < -0.3. Based on Fig. 6  
267 and 7, the significant correlation between precipitation and MJO-4 under NINO4 > 0 condition relative  
268 to ENSO in Table 1 is demonstrated in detail.

269 Fig. 7 Box-percentile plots of Canadian Prairies' precipitation anomaly during growing season versus MJO-4 under  
270 warm NINO4 (NINO4> 0, left) and cold NINO4 (NINO4<0, right) condition.

271 The strong correlation between MJO-4 and the prairie precipitation during growing season leads  
272 us to investigate the underlying circulation anomalies. Fig. 8 presents the regressed stream function and  
273 wind field at 200 hPa in the midlatitudes (north of 30N) on the negative MJO-4 index from May to  
274 August under warm NINO4 SST condition (NINO4 > 0.). In the tropics (10S-20N, considering it is  
275 during Northern Hemisphere summer), the OLR, velocity potential, and divergent wind vector are  
276 plotted. Only regression patterns have p-values lower than 0.05 are plotted for OLR and velocity  
277 potential. The negative MJO-4 index corresponds to a negative anomaly in OLR, stronger convection  
278 and larger than average divergence in the region centered on 150 E. The strong convection anomaly  
279 centers on 150 E, 5 N with divergent wind extending well into the subtropics in the Northern  
280 Hemisphere. The positive GPH/stream function anomaly extended from Japan to central Pacific is  
281 associated with the enhanced convection and divergence in the upper troposphere over the western  
282 tropical-subtropical Pacific. A Rossby wave train linked to the OLR anomaly and strong divergence in  
283 the western Pacific propagate eastward into North America. 

## 284 4 Discussion

285 The growing season precipitation in the Canadian Prairies are affected by many factors and  
286 precipitation deficit can occur under various circulation and lower boundary conditions. Thus it is not  
287 expected to find a universal condition for all the significant droughts in the region. In fact, extreme  
288 drought conditions have been found in both El Nino years and La Nina years. Though previous research  
289 by Bonsal and Lawford (1999) indicates the meteorological drought often occurs after the mature phase  
290 of El Nino, which is not the case for 2015, the associated changes in the North Pacific represented by

291 NPM positive phase is consistent with their results. The direct linkage between ENSO and the summer  
292 precipitation in the Canadian Prairies is still not clear. In fact, the correlation between MEI and  
293 precipitation in the investigated region is  $-0.096$  ( $p=0.2389$ , sample size = 152). It is not a significant  
294 correlation which is consistent with other researchers' findings (Dai and Wigley 2000).

295 The regression pattern is consistent with stationary Rossby wave theory as shown in a hierarchy  
296 of theoretical and modeling studies (Karoly *et al.* 1989, Simmons *et al.* 1983, Hoskins and Ambrizzi  
297 1993, Ambrizzi and Hoskins 1997, Held *et al.* 2002). A similar wave train extends from the western  
298 Pacific toward South America in the extratropics but at lower latitudes compared to its counterpart in the  
299 Northern Hemisphere (not shown). The node of the wave train in Western Canada and Northwest  
300 Pacific of the US corresponds to an anomalous ridge, which is in-phase of El Nino forcing. When the  
301 convection in the region associated with MJO-4 is weaker than normal ( $MJO-4 > 0$ ), a wave train with  
302 the opposite sign would reach western Canada which would counteract El Nino forcing. Thus, the  
303 weak correlation between Canadian Prairie precipitation and ENSO is understandable as MJO plays an  
304 additional role that enhances or cancels out the GPH anomaly caused by El Nino.

305 The atmospheric response in midlatitude North America to the tropical forcing in the western  
306 Pacific depends on the mean circulation condition associated with tropical SST. Intraseasonal tropical  
307 convection oscillation in the western Pacific associated with MJO-4 index cannot determine the sign of  
308 precipitation anomaly in the prairie. Both warm SST in central Pacific and strong tropical convection in  
309 western Pacific and Maritime Continent are necessary to cause a significant precipitation deficit in the  
310 western Canadian Prairies. Warm SST in central Pacific causes an eastward expansion of Pacific warm  
311 pool that favors enhanced MJO activity in the western-central Pacific (Hendon *et al.* 1999, Marshall *et*  
312 *al.* 2016). For the year of 2015, while the anomalous positive GPH associated with strong negative  
313 MJO4 indices in addition to the SST anomaly in the Pacific (e.g. ENSO, NPM) forced the anomalous

314 ridge on the west coast of Canada which reduces precipitation in the Canadian Prairies in the early  
315 summer. Although the El Niño continued to strengthen in July and August 2015, the active convections  
316 associated with MJO in West Pacific propagated eastward into the central Pacific, as the convection in  
317 the western Pacific/Maritime Continent waned, the precipitation in the Canadian Prairie returned to  
318 slightly above normal in July.

319 Fig. 8 The regression of stream function, wind field in the extratropics on MJO-4 for May-August with MEI > 0.5.  
320 Bottom: OLR, velocity potential, and divergent wind in the tropics on MJO-4 indices for May-August with *NINO4* > 0. The  
321 shaded region for the tropical OLR has p-value < 0.05. Blue shading indicates active convection region. Red dashed contour  
322 and solid blue contour corresponds to negative and positive velocity potential, respectively.

## 323 **5 Conclusions**

324 The cause of the summer precipitation deficit in the western Canadian Prairies is investigated  
325 regarding atmospheric circulation anomalies, sea surface temperature, and intraseasonal tropical  
326 convection oscillation, MJO. The drought in western Canada is immediately related to the anomalous  
327 ridge in the upper-level. The persistent anomalous upper-level ridge hovering around the west coast of  
328 Canada and Alaska since fall 2014 is likely associated with SST anomaly in the tropical (ENSO) and  
329 extratropical Pacific (NPM) as both SST patterns tend to associate with an anomalous high in Alaska  
330 and western Canada. However, the anomalous ridge itself explains the drought in the western Canada,  
331 the underlying cause of the anomalous ridge and whether it is related to ENSO need investigation . After  
332 all the significant deficit of precipitation concentrated in May and June 2015 when El Niño was still  
333 growing in intensity. The correlation of ENSO with the prairie precipitation is also not significant during  
334 summer. Instead, the intraseasonal oscillation in tropical convection, MJO, plays an important role in  
335 determining precipitation anomaly during months with warm central Pacific SST (*NINO4* > 0).

336 In general, MJO-4 indices demonstrate significant correlation with the meteorological drought  
337 from May to August with warm SST in central Pacific (NINO4 >0) when MJO amplitude is also often  
338 stronger. The new finding in our investigation is that MJO phase/strength is connected to the anomalous  
339 ridge in Western Canada when NINO4 is positive through the propagation of stationary Rossby wave  
340 from the western Pacific. The connection between the Canadian Prairie precipitation deficit and MJO is  
341 stronger when NINO4 is positive because MJO amplitude is stronger when the central Pacific SST is  
342 warmer than normal (NINO4 >0). The underlying cause of this significant correlation between MJO-4  
343 indices and the prairie precipitation in May-August is a stationary Rossby wave train originates from  
344 Maritime Continent and western Pacific and propagate into Canada. The intra-seasonal predictability in  
345 MJO amplitude and phase can be potentially instrumental for medium-range/intra-seasonal projection of  
346 the growing season precipitation in the Canadian Prairies when the central-Pacific SST is warm.

347

## 348 **Acknowledgement**

349 We gratefully acknowledge the Natural Sciences and Engineering Research Council of Canada  
350 (NSERC) for funding the Changing Cold Regions Network (CCRN) through their Climate Change and  
351 Atmospheric Research (CCAR) Initiative. Dr. Zhenhua Li is supported by the Probing the Atmosphere  
352 of the High Arctic project sponsored by the NSERC. This research is also supported by Environment and  
353 Climate Change Canada (ECCC). Dr. Y. Li gratefully acknowledges the support from the Global  
354 Institute of Water Security at the University of Saskatchewan.

355 **References**

- 356 Ambrizzi T and Hoskins B J 1997: Stationary Rossby-Wave Propagation in a Baroclinic Atmosphere,  
357 *Quart. J. Roy. Meteor. Soc.*, **123** 919–28.
- 358 Andrews, E.D., R.C. Antweiler, P.J. Neiman, and F.M. Ralph 2004 Influence of ENSO on Flood  
359 Frequency along the California Coast. *J. Climate*, **17**, 337–348, doi: 10.1175/1520-0442(2004)017.
- 360 Bonsal, B.R., Chakravarti, A.K. and Lawford, R.G. 1993: Teleconnections between North Pacific SST  
361 Anomalies and Growing Season Extended Dry Spells on the Canadian Prairies, *Int. J. Climatol.*, **13**,  
362 865-878.
- 363 Bonsal, B.R., Zhang, X. and Hogg, W.D., 1999: Canadian Prairie growing season precipitation  
364 variability and associated atmospheric circulation, *Climate Research*, **11**(3), 191-208.
- 365 Bonsal B and Lawford R 1999: Teleconnections between El Niño and La Niña Events and Summer  
366 Extended Dry Spells on the Canadian Prairies, *International Journal of Climatology*, **19**, 1445–58.
- 367 Bonsal B R, Shabbar A and Higuchi K, 2001: Impacts of Low Frequency Variability Modes on  
368 Canadian Winter Temperature, *Int. J. Climatol.* **21**, 95–108.
- 369 Bonsal B R and Regier M, 2007: Historical Comparison of the 2001/2002 Drought in the Canadian  
370 Prairies, *Climate Research*, **33**, 229-242.
- 371 Bonsal, B R, Aider, R, Gachon, P and Lapp S, 2013: An Assessment of Canadian Prairie Drought: Past,  
372 Present, and Future, *Climate Dynamics*, **41**, 501–516.
- 373 Carbone R. E., Yanping Li, 2015: Tropical Oceanic Rainfall and Sea Surface Temperature Structure:  
374 Parsing Causation from Correlation in the MJO, *Journal of Atmospheric Science*, Vol. 72, No. 7, 2703–  
375 2718.
- 376 Cassou C, 2008: Intraseasonal Interaction Between the Madden-Julian Oscillation and the North  
377 Atlantic Oscillation, *Nature*, **455** 523–7.

378 Dai A and Wigley T M L, 2000: Global Patterns of ENSO-Induced Precipitation, *Geophys. Res. Lett.*,  
379 **27** 1283–6.

380 Dee D P, Uppala S M, Simmons A J, Berrisford P, Poli P, Kobayashi S, Andrae U, Balmaseda M A,  
381 Balsamo G, Bauer P, Bechtold P, Beljaars A C M, Berg L van de, Bidlot J, Bormann N, Delsol C,  
382 Dragani R, Fuentes M, Geer A J, Haimberger L, Healy S B, Hersbach H, Hólm E V, Isaksen L, Kållberg  
383 P, Köhler M, Matricardi M, McNally A P, Monge-Sanz B M, Morcrette J-J, Park B-K, Peubey C,  
384 Rosnay P de, Tavolato C, Thépaut J-N, and Vitart F, 2011: The ERA-Interim Reanalysis: Configuration  
385 and Performance of the Data Assimilation System, *Quarterly Journal of the Royal Meteorological*  
386 *Society*, **137**, 553–97.

387 Dey B, 1982: Nature and Possible Causes of Droughts on the Canadian Prairies-Case Studies, *Journal of*  
388 *Climatology*, **2**, 233–49.

389 Garfinkel C I, Feldstein S B, Waugh D W, Yoo C and Lee S, 2012: Observed Connection Between  
390 Stratospheric Sudden Warmings and the Madden-Julian Oscillation, *Geophys. Res. Lett.*, **39**.

391 Hartmann D L, 2015: Pacific Sea Surface Temperature and the Winter of 2014, *Geophys. Res. Lett.*, **42**,  
392 1894–902.

393 Held I. M., Ting M. and Wang H., 2002: Northern Winter Stationary Waves: Theory and Modeling *J.*  
394 *Climate*, **15**, 2125–44.

395 Hendon, H. H., C. Zhang, and J. D. Glick, 1999: Interannual variation of the Madden-Julian Oscillation  
396 during Austral summer, *J. Clim.*, 12, 2538–2550

397 Hong, C. C., Hsu, H. H., Tseng, W.-L., Lee, M. Y., Chow, C.-H., & Jiang, L.-C. 2017: Extratropical  
398 Forcing Triggered the 2015 Madden–Julian Oscillation–El Niño Event. *Sci. Rep.* **7**, 46692; doi:  
399 10.1038/srep46692.

401 Hoskins B J and Ambrizzi T, 1993: Rossby Wave Propagation on a Realistic Longitudinally Varying  
402 Flow. *J. Atmos. Sci.* **50** 1661–71

403 Huang B, Banzon V F, Freeman E, Lawrimore J, Liu W, Peterson T C, Smith T M, Thorne P W,  
404 Woodruff S D and Zhang H-M, 2015: Extended Reconstructed Sea Surface Temperature Version 4  
405 (ERSST. v4). Part I: Upgrades and Intercomparisons *Journal of Climate*, **28** ,911–30.

406 Kalnay E, Kanamitsu M, Kistler R, Collins W, Deaven D, Gandin L, Iredell M, Saha S, White G,  
407 Woollen J, Zhu Y, Chelliah M, Ebisuzaki W, Higgins W, Janowiak J, Mo K, Ropelewski C, Wang J,  
408 Leetmaa A, Reynolds R, Jenne R and Joseph D, 1996: The NCEP/NCAR 40-Year Reanalysis Project  
409 *Bull. Amer. Meteor. Soc.* **77** 437–71

410 Karoly D J, Plumb R A, and Ting M, 1989: Examples of the Horizontal Propagation of Quasi-Stationary  
411 Waves. *J. Atmos. Sci.* **46** 2802–11

412 Lee M Y, Hong C C and Hsu H H 2015: Compounding Effects of Warm Sea Surface Temperature and  
413 Reduced Sea Ice on the Extreme Circulation Over the Extratropical North Pacific and North America  
414 During the 2013/2014 Boreal winter *Geophys. Res. Lett.*, **42**, 1612–8.

415 Yanping Li, Richard E. Carbone, 2012: Excitation of rainfall over the tropical western Pacific. *Journal*  
416 *of Atmospheric Science*, Vol. 69, No. 10, 2983–2994.

417 Yanping Li, Kit Szeto, Ron Stewart, Julie Theriault, Liang Chen, Bob Kochtubajda, Anthony Liu,  
418 Sudesh Boodoo, Ron Goodson, Curtis Mooney, Sopan Kurkute, 2017: The June 2013 Alberta  
419 Catastrophic Flooding: Water vapor transport analysis by WRF simulation. *Journal of*  
420 *Hydrometeorology*, Vol. 18, 2057-2078.

421 Zhenhua Li, Alan Manson, Yanping Li, Chris Meek, 2017: Circulation Characteristics of Persistent  
422 Cold Spells in Central-Eastern North America. *Journal of Met. Res.*, Vol. 31, 250-260.

423 Liu J, Stewart R E and Szeto K K, 2004: Moisture Transport and Other Hydrometeorological Features  
424 Associated With the Severe 2000/01 Drought Over the Western and Central Canadian Prairies *Journal*  
425 *Of Climate*, **17**, 305–19.

426 Lorenz, D.J. and D.L. Hartmann, 2006: The Effect of the MJO on the North American Monsoon. *J.*  
427 *Climate*, **19**, 333–343, doi: 10.1175/JCLI3684.1.

428 Madden R A and Julian P R, 1971: Detection of a 40-50 Day Oscillation in the Zonal Wind in the  
429 Tropical Pacific, *J. Atmos. Sci.*, **28**, 702–8

430 Marshall, A. G., H. H. Hendon, and G. Wang, 2016: On the role of anomalous ocean surface  
431 temperatures for promoting the record Madden-Julian Oscillation in March 2015, *Geophys. Res. Lett.*,  
432 43,472–481.

433 Riddle E E, Stoner M B, Johnson N C, L’Heureux M L, Collins D C and Feldstein S B, 2013: The  
434 Impact of the MJO on Clusters of Wintertime Circulation Anomalies Over the North American region  
435 *Climate Dynamics*, **40**, 1749–66.

436 Rodney, M., Lin, H., & Derome, J. 2013: Subseasonal Prediction of Wintertime North American  
437 Surface Air Temperature during Strong MJO Events. *Monthly Weather Review*, *141*(8), 2897–2909.  
438 <http://doi.org/10.1175/MWR-D-12-00221.1>.

439 Ropelewski C F and Halpert M S 1986: North American Precipitation and Temperature Patterns  
440 Associated with the El Niño/Southern Oscillation (ENSO), *Monthly Weather Review*, **114**, 2352–62.

441 Shabbar, A., Bonsal, B. and Khandekar, M., 1997: Canadian precipitation patterns associated with the  
442 Southern Oscillation. *Journal of Climate* 10:3016-3027.

443 Shabbar A and Skinner W, 2004: Summer Drought Patterns in Canada and the Relationship to Global  
444 Sea Surface Temperatures, *Journal of Climate*, **17**, 2866–80.

445 Shabbar A, Bonsal B R and Szeto K, 2011: Atmospheric and Oceanic Variability Associated with  
446 Growing Season Droughts and Pluvials on the Canadian Prairies, *Atmosphere-Ocean*, **49**, 339–55.

447 Simmons A J, Wallace J M and Branstator G W, 1983: Barotropic Wave Propagation and Instability,  
448 and Atmospheric Teleconnection Patterns, *J. Atmos. Sci.*, **40**, 1363–92.

449 Szeto, K., X. Zhang, R.E. White, and J. Brimelow, 2016: The 2015 Extreme Drought in Western  
450 Canada. *Bull. Amer. Meteor. Soc.*, **97**, S42–S46, <https://doi.org/10.1175/BAMS-D-16-0147.1>.

451 Wang S Y, Hipps L, Gillies R R and Yoon J-H, 2014: Probable Causes of the Abnormal Ridge  
452 Accompanying the 2013-2014, California Drought: ENSO Precursor and Anthropogenic Warming  
453 footprint *Geophys. Res. Lett.*, **41** 3220–6.

454 Xie P and Arkin P A, 1997: Global Precipitation: A 17-year Monthly Analysis Based on Gauge  
455 Observations, Satellite Estimates, and Numerical Model Outputs. *Bulletin of the American*  
456 *Meteorological Society*, **78**, 2539–58.

457 Xue Y, Higgins W and Kousky V 2002: Influences of the Madden-Julian Oscillations on Temperature  
458 and Precipitation in North America during ENSO-neutral and Weak ENSO Winters, *Proc. workshop on*  
459 *prospects for improved forecasts of weather and short-term climate variability on subseasonal (2 week*  
460 *to 2 month) time scales*.

461 Wheaton, E, Wittrock V, Kulshreshtha S, Koshida G, Grant C, Chipanshi A, Bonsal BR, 2005: Lessons  
462 Learned from the Drought Years of 2001 and 2002: Synthesis Report. Agriculture and Agri-Food  
463 Canada, Saskatchewan Research Council Publ No. 11602–46E03, Saskatoon.

464 Wheeler, M. C., & Hendon, H. H., 2004: An all-season real-time multivariate MJO index: Development  
465 of an index for monitoring and prediction. *Monthly Weather Review*, *132*(8), 1917–1932.

466 Wolter, K., 1987: The Southern Oscillation in surface circulation and climate over the tropical  
467 Atlantic, Eastern Pacific, and Indian Oceans as captured by cluster analysis. *J. Climate Appl.*  
468 *Meteor.*, 26, 540-558.

469 Wolter, K. and M.S. Timlin, 1993: Monitoring ENSO in COADS with a seasonally adjusted principal  
470 component index. Proc. of the 17th Climate Diagnostics Workshop, Norman, OK,  
471 NOAA/NMC/CAC, NSSL, Oklahoma Clim. Survey, CIMMS and the School of Meteor., Univ. of  
472 Oklahoma, 52-57.

473 Zhang C, 2005: Madden-Julian Oscillation *Reviews of Geophysics*, **43**.

474

475

476

477

478

479

480

481

482

483

484

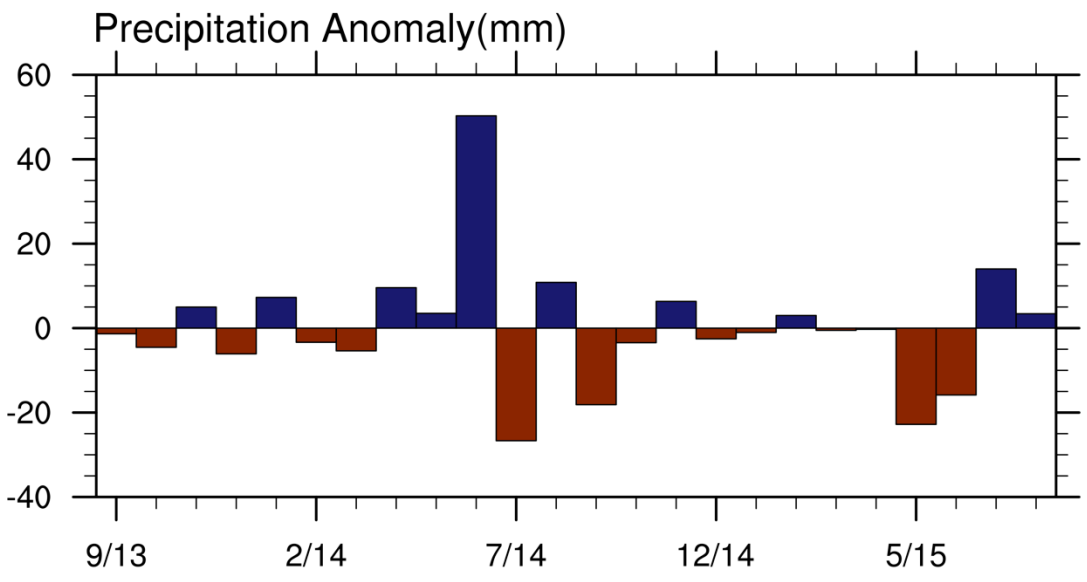
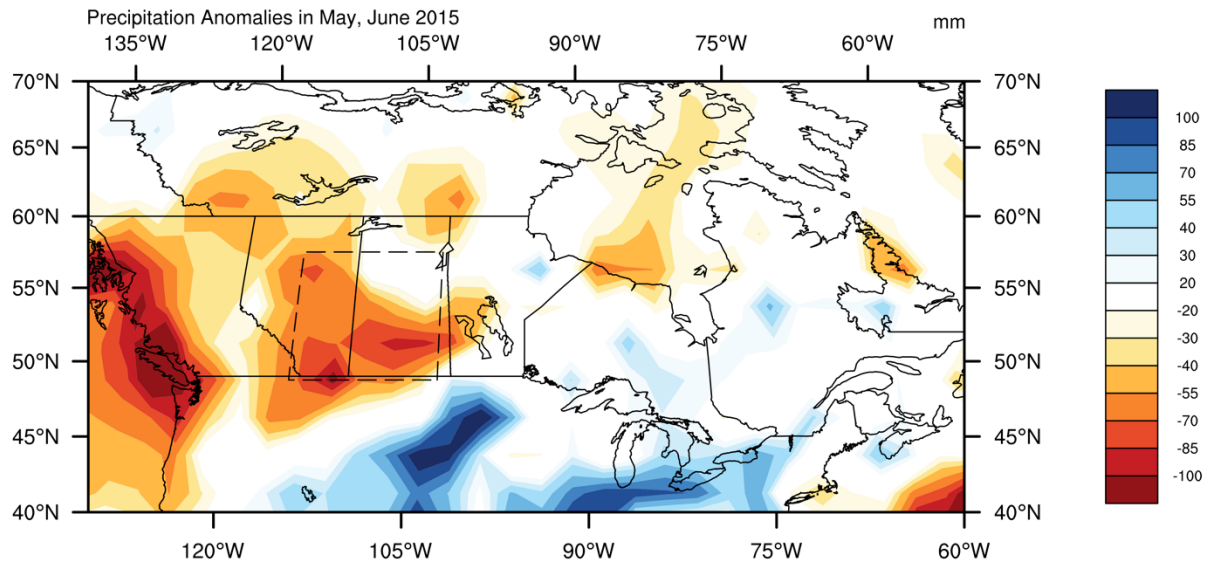
485

486 Table 1 Correlation between mean precipitation anomaly from CMAP in the prairie and MEI, MJO

487 indices 4. MJO indices and are from 1979 to 2016. CMAP covers 1979 to 2016.

	Correlation	p-value	No. of sample
MEI	-0.096	0.24	156
MJO-4	0.18	0.023	156
MJO-4(NINO4>0)	0.33	0.0015	90
MJO-4(NINO4<0)	-0.01	0.94	66

488



489  
 490 Fig. 1 Top: Precipitation anomalies (mm) from CMAP over the region (115 W-102.5 W, 50 N-57.5 N)  
 491 during May and June 2015. Bottom: time series of monthly precipitation anomaly over boxed region  
 492 between September 2013 and August 2015.

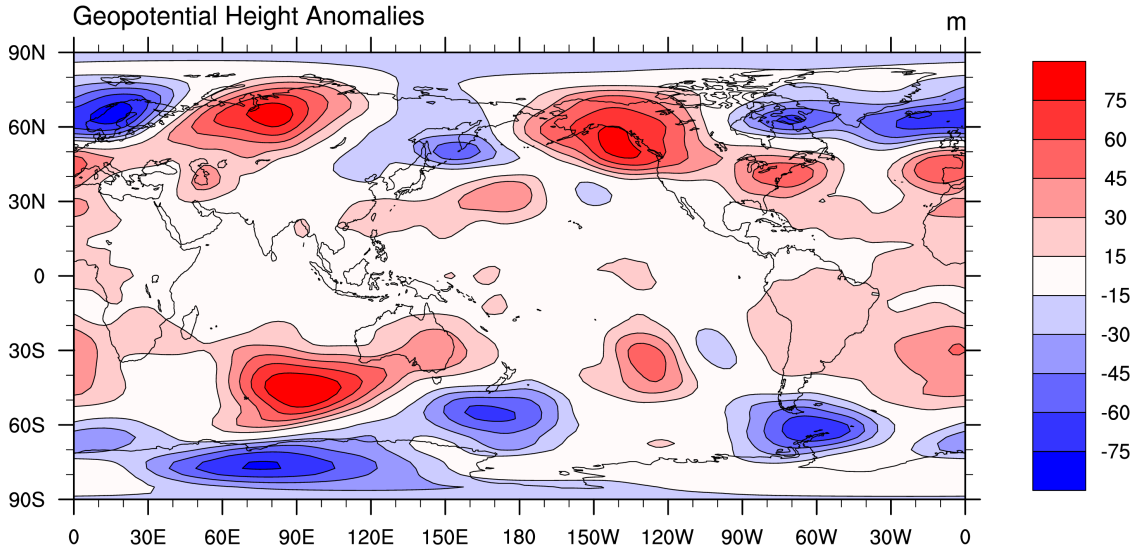
493  
 494

495

496

497

### Mean GPH Anomaly of May, June 2015



498

499 Fig. 2 NCEP GPH anomaly at 500hPa during May and June 2015 when the precipitation deficit was the  
500 largest.

501

502

503

504

505

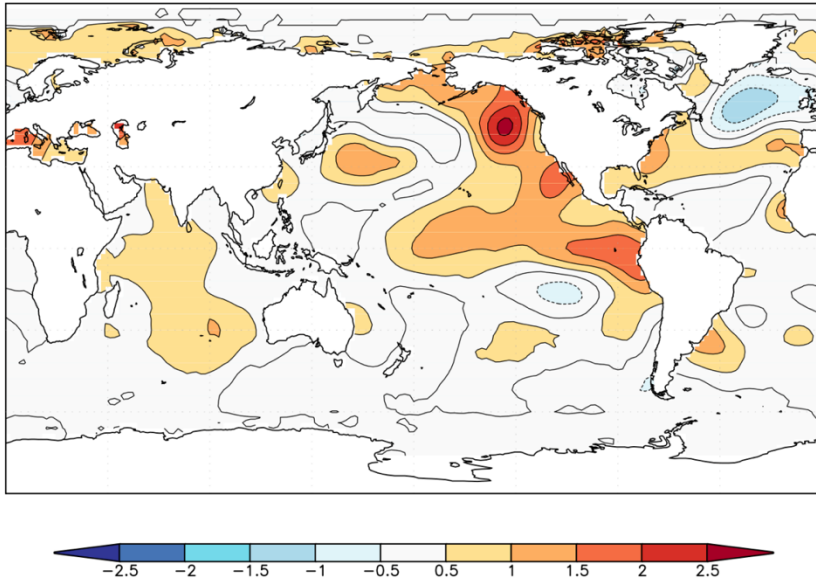
506

507

508

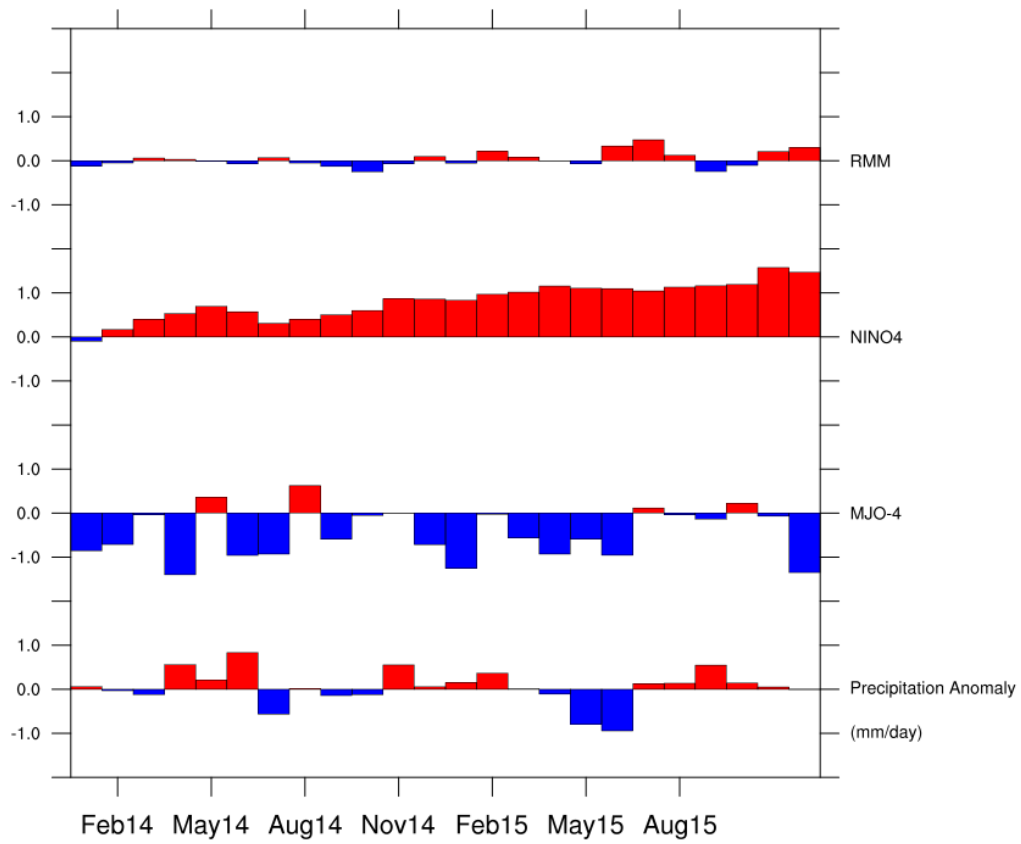
509

510



511

512 Fig. 3 The mean SST anomaly(°C) from ERSST v4 in May-August 2015.



513

514 Fig. 4 RMM amplitude anomaly, NINO4, MJO 4 indices and precipitation anomaly of Canadian Prairies  
 515 from January 2014 to Dec 2015.

516

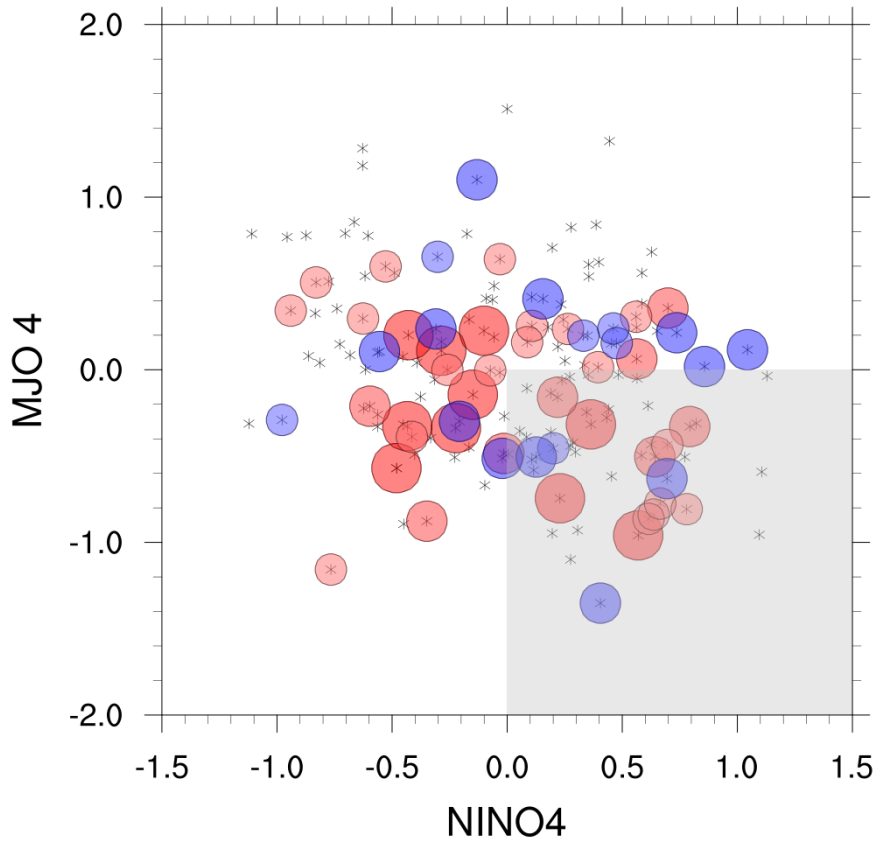
517

518

519

520

521



522

523

524

525

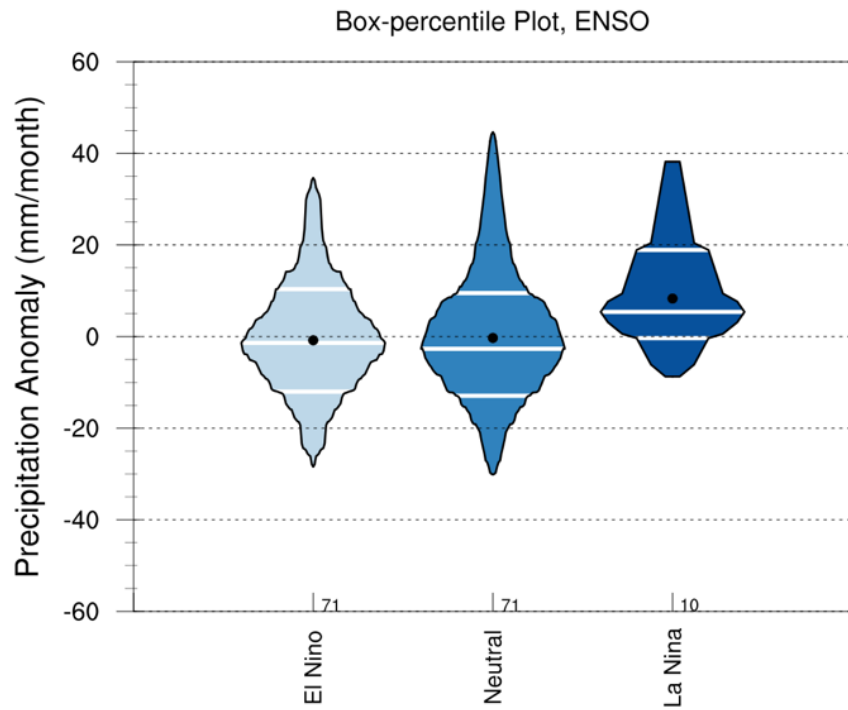
526

527

528

529

Fig. 5 The scatterplot of monthly precipitation anomaly (mm/month) as a function of MJO-4 and NINO4. Each asterisk represents a month from May to August 1979-2016. Circled asterisk denotes a month with precipitation anomaly larger than 18 mm/month. The blue circles are months with positive precipitation anomaly and the red circles are months with negative precipitation anomaly. The sizes of circles denote the magnitudes of the anomalies (large > 30 mm/month, medium > 24 mm/month, small > 18 mm/month). The shaded area denotes NINO4 > 0 and MJO-4 index < 0.



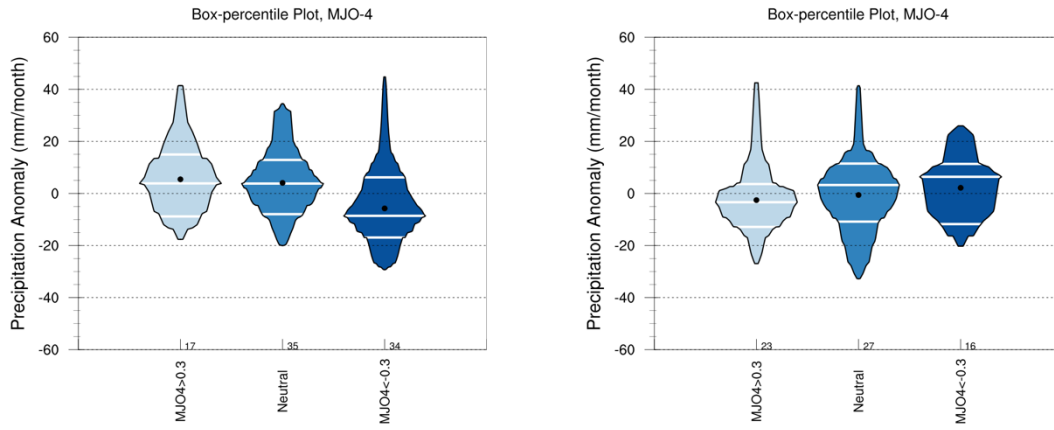
530

531 Fig. 6 The box-percentile plot of Canadian Prairies precipitation anomaly during growing season for  
532 ENSO conditions.

533

534

535



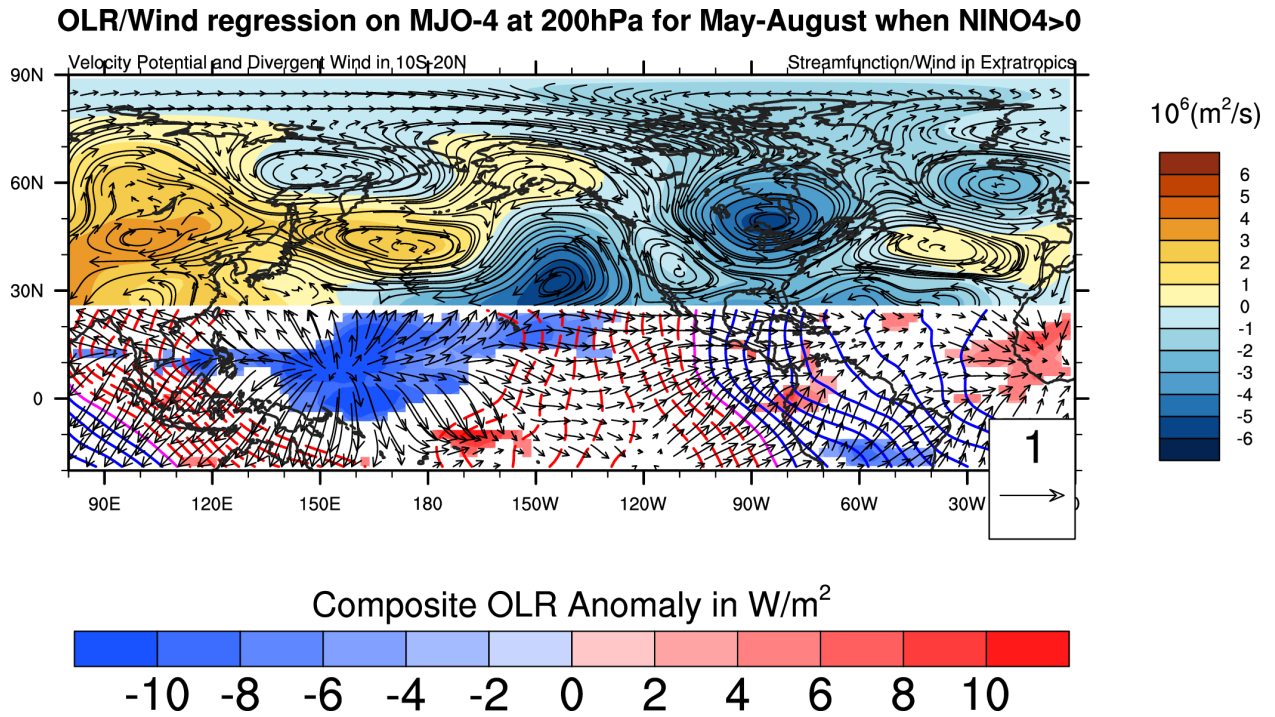
536

537 Fig. 7 Box-percentile plots of Canadian Prairies' precipitation anomaly during growing season

538 versus MJO-4 under warm NINO4 (NINO4 > 0, left) and cold NINO4 (NINO4 < 0, right) condition.

539

540



541

542

543

544

545

546

547

548

549

550

Fig. 8 The regression of stream function, wind field in the extratropics on MJO-4 for May-August with MEI > 0.5. Bottom: OLR, velocity potential, and divergent wind in the tropics on MJO-4 indices for May-August with *NINO4* > 0. The shaded region for the tropical OLR has p-value < 0.05. Blue shading indicates active convection region. Red dashed contour and solid blue contour corresponds to negative and positive velocity potential, respectively.